PAPER

Leaking of trajectories from the phase space of discontinuous dynamics

IOP Publishing Journal of Physics A: Mathematical and Theoretical
J. Phys. A: Math. Theor. **48** (2015) 405101 (10pp) doi:10.1088/1751-8113/48/40/405101

Leaking of trajectories from the phase space of discontinuous dynamics

J A Méndez-Bermúdez[1], A J Martínez-Mendoza[1], André L P Livorati[2] and Edson D Leonel[2,3]

[1] Instituto de Física, Benemérita Universidad Autónoma de Puebla, Apartado Postal J-48, Puebla 72570, Mexico
[2] Departamento de Física, UNESP—Univ Estadual Paulista, Av. 24A, 1515, Bela Vista, 13506-900 Rio Claro, SP, Brazil
[3] Abdus Salam International Center for Theoretical Physics, Strada Costiera 11, 34151 Trieste, Italy

E-mail: jmendezb@ifuap.buap.mx

Received 10 April 2015, revised 29 July 2015
Accepted for publication 13 August 2015
Published 14 September 2015

Abstract

The escape of particles from the phase space produced by a two-dimensional, nonlinear and area-preserving, discontinuous map is investigated by using both numerical simulations and the explicit solution of the corresponding diffusion equation. The mapping, given in action-angle variables, is parameterized by K, which controls a transition from integrability to non-integrability. We focus on the two dynamical regimes of the map: slow diffusion ($K < K_c$) and quasilinear diffusion ($K > K_c$) regimes, separated by the critical parameter value $K_c = 1$. When a hole is introduced in the action axis, we find the histogram of escape times $P_E(n)$ and the survival probability of particles $P_S(n)$ to be scaling invariant in both the slow and the quasilinear diffusion regimes, with scaling laws proportional to the corresponding diffusion coefficients, namely, proportional to $K^{5/2}$ and K^2, respectively. Our numerical simulations agree remarkably well with the analytical results obtained from the explicit solution of the diffusion equation, hence giving robustness to the escape formalism.

Keywords: escape formalism, diffusion, scaling

(Some figures may appear in colour only in the online journal)

1. Introduction

A scattering design composed of a dynamical system (serving as a target) which is connected to an asymptotic region by a hole or leak has been shown to be a useful setup to probe

dynamical properties of the target system by the use of transport or scattering quantities [1]. For classical systems the leak can be a physical hole (such as an opening in the boundary of a billiard table) or a subset of the phase space (i.e., a threshold in one of the variables). In either case a trajectory, with initial conditions inside the system, that reaches the hole is considered to escape from the system[4]. Indeed, following an ensemble of trajectories and counting the number of them still inside the system up to time t defines the survival probability $P(t)$. $P(t)$ is known to decay exponentially for strongly chaotic systems and develops, due to stickiness, asymptotic power-law tails in the case of mixed-chaotic dynamics [1, 2].[5]

Most studies of classical leaking focus on systems whose dynamics is in one of the stages of the generic transition to chaos (also known as Kolmogorov–Arnold–Moser (KAM) scenario): Integrable dynamics [4], mixed-chaotic dynamics [2, 3], and full chaos [5–7] (indeed, in the latter case, the development of power-law tails in $P(t)$ uncovers the presence of minuscule stability islands embedded in a seemingly ergodic phase space [8].) The prototype model used to study KAM systems is Chirikov's standard map (CSM) [9–11]. However, there is a family of dynamical systems for which KAM theorem is not satisfied. This family is characterized by *discontinuous maps* whose corresponding dynamics exhibits unbounded diffusion [12, 13]. Among the systems whose dynamics can be described by discontinuous maps we mention the Bunimovich stadium billiard [14, 15] (where the corresponding *stadium map* was constructed to study diffusion in angular momentum), the triangular billiard [16, 17], which in turn is equivalent to the motion of three particles on a ring with their masses connected to the angles of a triangle [18], and the sawtooth map [19]. To the best of our knowledge, leaking from systems developing discontinuous dynamics has not been approached yet. Therefore, in this paper we undertake this task by considering the escape of trajectories from a generalized discontinuous map.

2. The map and its properties

The two-dimensional, nonlinear, and area preserving, discontinuous map we consider in this paper is written in terms of action and angle variables. It is given by [12]

$$\begin{cases} I_{n+1} = I_n + K \sin(\theta_n)\mathrm{sgn}\left[\cos(\theta_n)\right] \\ \theta_{n+1} = \left[\theta_n + I_{n+1}\right], \qquad \mathrm{mod}\ (2\pi) \end{cases}, \tag{1}$$

where K is a parameter controlling a transition from integrability to non-integrability. Map (1) is known to have two dynamical regimes, both diffusive, delimited by the critical value $K_c = 1$ [12]. The regimes $K < K_c$ and $K > K_c$ are known as slow diffusion and quasilinear diffusion regimes, respectively. As an example of the dynamics of map (1), in figure 1, we show typical Poincaré surface of sections in both regimes. Note that map (1) is very similar to CSM (the only difference is the presence of the sign function in the iteration relation for the action in (1)), which also shows two regimes separated by $K_c \sim 1$ [9–11, 20–23]. However, there is a fundamental difference between both maps: For $K < K_c$ the discontinuous map does not show regular behavior. In fact, due to discontinuities, the KAM theorem is not satisfied and map (1) does not develop the KAM scenario. Since for any $K \neq 0$ the dynamics of map (1) is diffusive, a single trajectory can explore the entire phase space. Moreover, in the

[4] In fact, the leaking problem is not restricted to a single hole in the system: by considering two or several holes the scattering setup can also be used to measure scattering quantities, such as transmission and reflection probabilities. In such case, the initial conditions of the corresponding trajectories may lie in the asymptotic region; i.e. outside the dynamical target system.

[5] An unexpected situation has been reported in [3] where, due to Fermi acceleration, $P(t)$ was shown to decay as a stretched exponential.

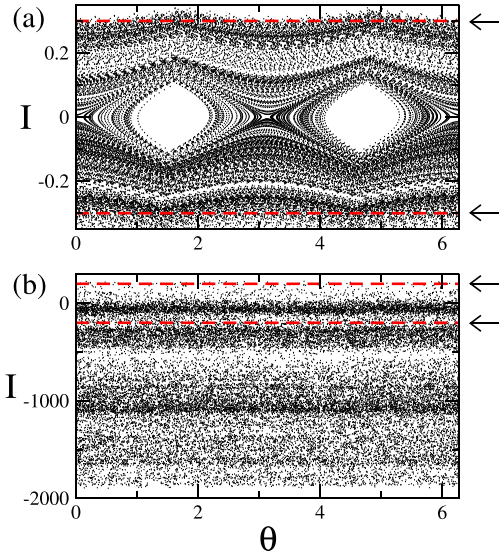

Figure 1. Poincaré surfaces of section for the discontinuous map of equation (1) with (a) $K = 0.01$ (slow diffusion regime) and (b) $K = 10$ (quasilinear diffusion regime). A single initial condition with $\theta_0 = 3$ and $I_0 = 0.01$ was iterated 3×10^4 times. Red dashed lines and arrows indicate the position of holes in the action axis at $I = \pm h$ with (a) $h = 0.3$ and (b) $h = 200$.

slow diffusion regime the dynamics is far from being stochastic due to the sticking of trajectories along cantori (fragments of KAM invariant tori), see e.g. figure 1(a). For $K > K_c$ map (1) shows diffusion similar to that of CSM.

We *open* the discontinuous map (1) by placing a *hole* on a subset of the phase space of constant action. Moreover, since the phase space of (1) is symmetric (i.e. $\langle I_n \rangle = 0$) we define the hole as two horizontal lines at $I = \pm h$ in the Poincaré maps. As examples, in figures 1(a) and (b) we show (as red-dashed lines, also indicated by arrows) holes with $h = 0.3$ and $h = 200$, respectively. Therefore, we analyze the escape of trajectories from map (1) as a function of the parameters K and h, controlling the nonlinearity of the map and the openness of the scattering setup, respectively.

In the next section, we approach the problem of leaking of trajectories from the phase space of discontinuous dynamics as follows: first, we analytically solve the diffusion equation concerning the escape formalism [8]. Our numerical and analytical results are in good agreement in both dynamical regimes, $K < K_c$ and $K > K_c$, where the obtained diffusion coefficients coincide with the ones reported in previous papers [12, 14, 19]. This agreement confirms the robustness of the escape formalism, here applied to discontinuous dynamical systems, that could be extended to many other systems. Then, we focus on two scattering functions, the survival probability and the frequency of particle escape, that we numerically compute as a function of the discrete time n and also use to validate the scalings found for the diffusion coefficient.

3. Results and discussion

3.1. Diffusion coefficient

In many scenarios, one is not interested in the individual behaviour of an initial condition or particle but in the average properties of the system by considering ensembles of initial

conditions [8]. This is the main reason to apply statistical techniques to describe dynamical phenomena [24]. When considering a leaking into a physical system, i.e., a hole, or even a barrier [25, 26], one can define the probability of an ensemble of initial conditions to survive this leaking as $\rho(I, t)$; where I represents the action variable and t is the time. So we can write the particle flux as

$$j(I, t) = -D\nabla\rho(I, t), \tag{2}$$

where D is the diffusion coefficient. In addition, the conservation of particles leads to

$$\frac{\partial\rho(I, t)}{\partial t} = -\nabla \cdot j(I, t). \tag{3}$$

Thus, by combining equations (2) and (3) we obtain the diffusion equation

$$\frac{\partial\rho(I, t)}{\partial t} = D\nabla^2\rho(I, t). \tag{4}$$

Since we want to apply this diffusion equation to our mapping, the time should be measured as the iteration number n.

To solve equation (4), we use the method of separation of variables and write $\rho(I, n) = \Xi(I)T(n)$. Then, equation (4) takes the form $T'(n)\Xi(I) = D\Xi''(I)T(n)$, which can be written as

$$\frac{T'(n)}{T(n)} = D\frac{\Xi''(I)}{\Xi(I)} = -\gamma, \tag{5}$$

where γ is a constant which, indeed, is the decay rate of the survival probability; see next subsection.

The solution of equation (5) for the variable n is the exponential function

$$T(n) = C_1 e^{-\gamma n}, \tag{6}$$

where C_1 is a constant. Now, from the part of equation (5) related to the action we write

$$\frac{\Xi''(I)}{\Xi(I)} = -\frac{\gamma}{D} = -\eta^2. \tag{7}$$

Equation (7) is an ordinary second order differential equation with constant coefficients, so its solutions are given in terms of sines and cosines. By incorporating the boundary conditions $\rho(\pm h, n) = 0$ into equation (7) and considering only odd solutions, we end up with the condition $\eta I = l\pi/2$, where $l = 1, 3, 5, \ldots$. Since $\eta^2 = \gamma/D$, we obtain $D = (4\,h^2\gamma)/(l^2\pi^2)$. Therefore, a solution for $\rho(I, n)$, given as a sum of terms in l reads [27]

$$\rho(I, n) = \sum_{l=1,3,5,\ldots}^{\infty} A_l \cos\left(\frac{I\pi}{2\,h}l\right)\exp\left(-\frac{\pi^2\,Dn}{4\,h^2}l^2\right). \tag{8}$$

Since l appears quadratic in the exponential function of equation (8), the first term in the sum is the leading one. This term provides the first order estimation of the diffusion coefficient:

$$D = \frac{4\,h^2\gamma}{\pi^2}\,. \tag{9}$$

Notice that the derivation for the diffusion coefficient made above is very general and the discontinuous map parameter K, see equation (1), enters into equation (9) through γ. Therefore, we still have to discover the dependence of D on K. To this end we numerically evaluate D for several values of K, in the slow diffusion and the quasilinear diffusion regimes of our map, and look for the corresponding power-law behaviors. That is, for a given K we

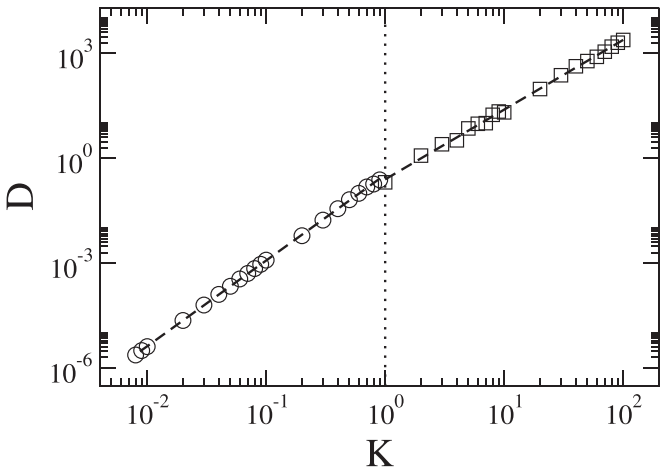

Figure 2. Diffusion coefficient D, computed from equation (9), as a function of K. Dashed lines are the best fits of the data with the power-law function $D \propto K^z$ with $z = 2.455(6)$ for $K < 1$ and $z = 1.996(2)$ for $K \geqslant 1$. $h = \pm 1$ and $h = \pm 1000$ were used for $K < 1$ and $K \geqslant 1$, respectively. The dotted vertical line separates the slow diffusion regime ($K < 1$) from the quasilinear diffusion regime ($K \geqslant 1$).

consider an ensemble of 10^6 initial conditions (with $I_0 = 0.01\,K$ and $\theta_0 \in [\pi - \delta, \pi + \delta]$, where $\delta = 0.0001$) and numerically construct $\rho(I, n)$; then, we extract the corresponding value of γ by the fitting of $\rho(I, n)$ with equation (8) and evaluate D from equation (9).

Figure 2 shows the behaviour of the diffusion coefficient as a function of K. The power-law behaviour

$$D \propto K^z \tag{10}$$

can clearly be observed, however, with an inflection point at the critical value $K_c = 1$. Indeed, power-law fittings to the data provide $z \approx 5/2$ for $K < K_c$ and $z \approx 2$ for $K > K_c$. We stress that the power-law dependencies of the diffusion coefficient on the parameter K we obtained here are in perfect agreement with the ones reported in [12] from the numerical computation of $D = \lim_{n\to\infty}\langle I_n^2\rangle/n$ for the discontinuous mapping of equation (1). In addition, in [12], the dependence $\mathrm{D} \propto K^2$ for $K > K_c$ was analytically supported in terms of the random phase approximation [11]. The anomalous behavior $D \propto K^{5/2}$ for $K < K_c$, found in our map (1) but also in other discontinuous maps (e.g., the sawtooth map [19] and the stadium map [14]), was understood as an effect of the sticking of trajectories along cantori [12, 15]. Moreover, in [19] a theoretical interpretation of the exponent $z \approx 5/2$ was given by the use of a Markov model of transport based on the partition of the phase space into resonances.

3.2. Survival probability

One of the most popular quantities used in studies of leaking is the survival probability $P_{\mathrm{S}}(n)$. Fortunately, once we have the expression for $\rho(I, n)$ in equation (8) we can compute $P_{\mathrm{S}}(n)$ by integrating $\rho(I, n)$ over I in the range $[0, h]$. Moreover, by noticing that the leading term in equation (8) corresponds to $l = 1$ we can write

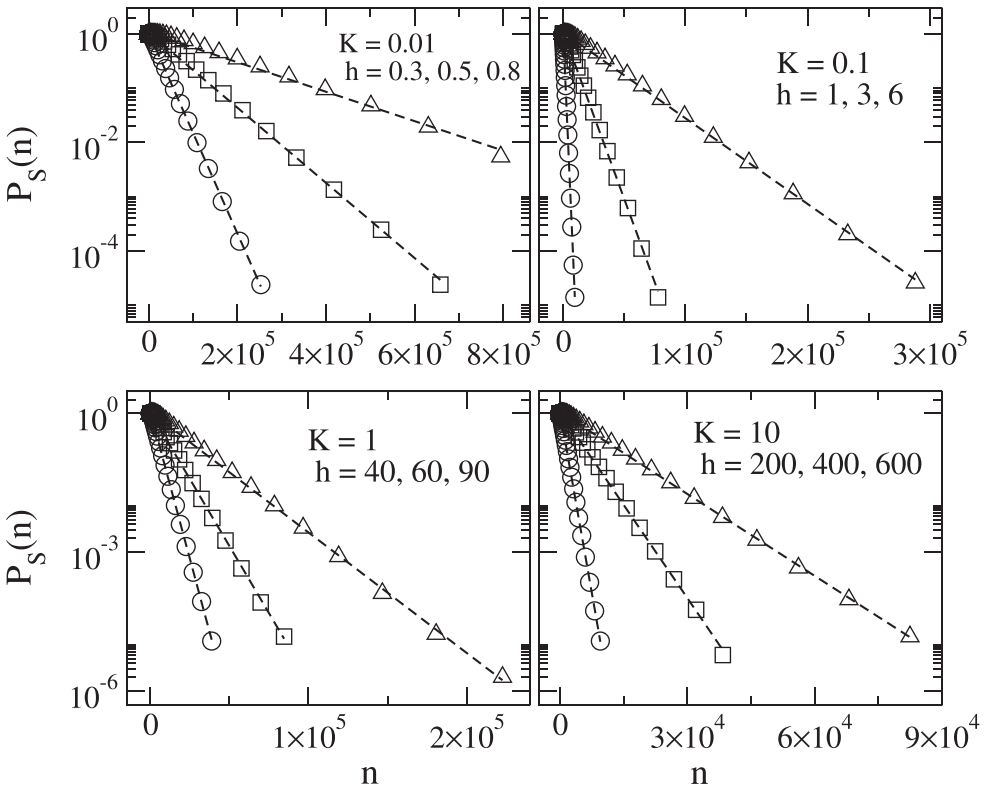

Figure 3. Survival probability $P_S(n)$ as a function of n for several combinations of K and h (symbols). Here, h increases from left to right. Dashed lines are fittings of the data with the exponentially-decaying function $\exp(-\mu n)$. Each curve was constructed by the use of $M = 10^6$ trajectories.

$$P_S(n) = \exp\left(-\frac{\pi^2 D}{4h^2}n\right), \tag{11}$$

where we have set $A_l = \pi/2h$ in order to recover the initial condition $P_S(0) = 1$.

Note that equation (11) predicts the exponential decay of the survival probability. Then, in order to verify this prediction we numerically compute the survival probability as

$$P_S(n) = \frac{1}{M}\sum_{j=1}^{M} N_S(n). \tag{12}$$

For each combination of parameters, K and h, we consider an ensemble of $M = 10^6$ trajectories all having the initial action $I_0 = 0$ and initial random phases θ_0 uniformly distributed in the interval $(0,\pi/2)$ (with this choice of θ_0 we avoid the period-one fixed points of the map at $I = 0$ and $\theta = [0, \pi/2, \pi, 3\pi/2, 2\pi]$). Each initial condition is evolved in time according to map (1). $N_S(n)$ in (12) is the number of trajectories that, at time n, have not escaped yet from the discontinuous map. Thus, in figure 3, we present $P_S(n)$ for several combinations of K and h. From this figure we observe that $P_S(n)$ shows a perfect exponential decay even for $K < 1$, where the non-ergodicity of the phase space, see figure 1(a), is assumed to be produced by the *sticking* of trajectories along cantori.

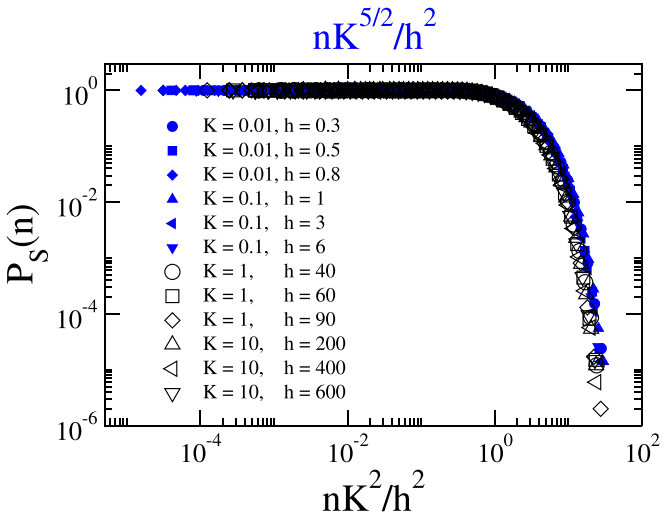

Figure 4. Scaled survival probability curves $P_S(n)$ as a function of $nK^{5/2}/h^2$ (blue full symbols) and nK^2/h^2 (black hollow symbols) for $K < 1$ and $K \geqslant 1$, respectively. Here we used the data curves from figure 3.

It is relevant to stress that due to the presence of the diffusion coefficient D in the expression for the survival probability, see equation (11), the scalings $D \propto K^{5/2}$ and $\mathrm{D} \propto K^2$ found for our discontinuous map in the slow diffusion and quasilinear diffusion regimes, respectively, could be confirmed using plots of $P_S(n)$. Indeed, we verify this hypothesis by a scaling analysis in figure 4. There, we plot the survival probability curves shown in figure 3 but now as a function of $nK^{5/2}/h^2$ (blue full symbols) and nK^2/h^2 (black hollow symbols) for $K < 1$ and $K \geqslant 1$, respectively. We observe that the curves $P_S(n)$ fall one on top of two slightly different universal curves: one for $K < 1$ and another for $K \geqslant 1$. In fact, these universal curves can be well-fitted by the bare exponential function $P(x) = \exp(-\mu x)$ where $x = nK^{5/2}/h^2$ [$x = nK^2/h^2$] when $K < 1$ [$K \geqslant 1$] with $\mu \approx 0.4$ [$\mu \approx 0.5$] (the fitting curves are not shown to avoid the saturation of figure 4).

3.3. Frequency of escape

A well-known quantity, closely related to the survival probability, is the frequency of escape $P_E(n)$. To construct $P_E(n)$ we consider an ensemble of $M = 10^6$ trajectories having as initial conditions $I_0 = 0$ and θ_0 a random phase. Each initial condition is evolved in time according to map (1). If, along the orbit, the action surpasses the hole, we determine that the trajectory has escaped from the discontinuous map and a new initial condition is selected. By counting the total number of trajectories that have escaped up to (the discrete) time n, we construct the histogram for the frequency of escape $P_E(n)$. We noted that $P_E(n)$ increases as a function of n until it reaches a maximum at an iteration number n_P. Then it decreases and approaches zero asymptotically for $n \to \infty$. However, since to observe the complete increase and decrease of $P_E(n)$ exponentially large iteration times are needed, we construct $P_E(\ln n)$ instead. Then, in figures 5(a) and (b), we present $P_E(\ln n)$ for $K < 1$ and $K \geqslant 1$, respectively, for several combinations of K and h.

From figures 5(a) and (b), it is clear the value of n_P strongly depends on both K and h. Indeed, as can be seen in these figures, the histograms $P_E(\ln n)$ are displaced monotonically to

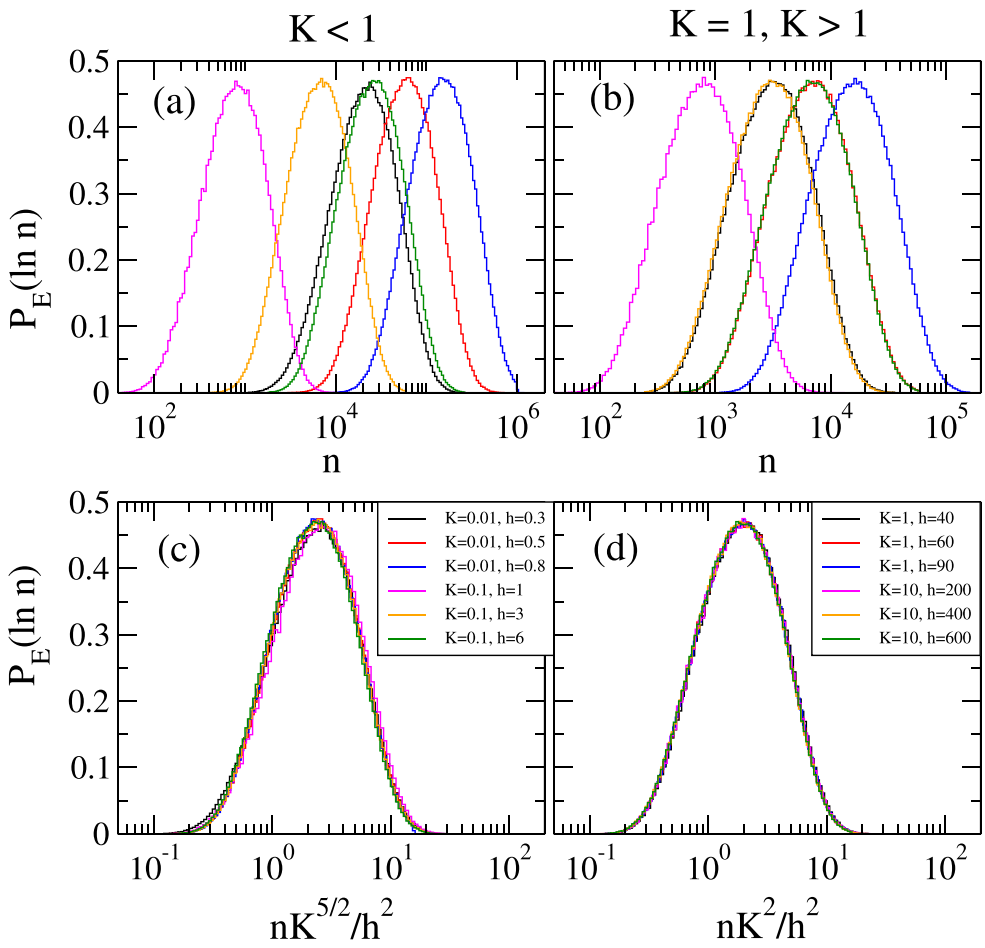

Figure 5. Histograms for the frequency of particle escape $P_E(\ln n)$ when (a) $K < 1$ and (b) $K \geqslant 1$ for several combinations of K and h. Scaled histograms $P_E(\ln n)$ as a function of (c) $nK^{5/2}/h^2$ and (d) nK^2/h^2. Each histogram was constructed by the use of $M = 10^6$ trajectories.

the right (to the left) when h (K) increases (decreases) for fixed K (h) in, both, the slow diffusion and the quasilinear diffusion regimes. Thus, we propose the following scaling hypotheses for n_P:

$$n_P \propto K^{\alpha_1} h^{\alpha_2}, \tag{13}$$

where α_1 and α_2 are scaling exponents. Therefore, in figure 6, we plot n_P versus K for several fixed values of h where the power-law behaviour $n_P \propto K^{\alpha_1}$ is clearly observed. However, it is relevant to stress that the scaling exponent α_1 depends on whether $K < 1$ or $K \geqslant 1$. In fact, we concluded that $\alpha_1 \approx -5/2$ for $K < 1$ while $\alpha_1 \approx -2$ for $K \geqslant 1$ (see the power-law fittings in figure 6). On the other hand by plotting now n_P versus h for fixed K (not shown here) we found that $\alpha_2 \approx 2$ in both regimes (slow diffusion and quasilinear diffusion). Therefore, in figures 5(c) and (d) we plot $P_E(\ln n)$ after the scalings $n \to nK^{5/2}/h^2$ when $K < 1$ and $n \to nK^2/h^2$ for $K \geqslant 1$, respectively, observing a

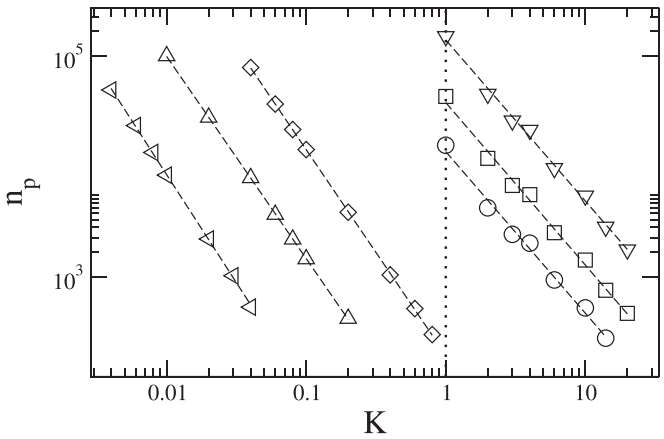

Figure 6. n_{P} (iteration time corresponding to the maximum of $P_{\mathrm{E}}(\ln n)$) as a function of K for $h = 0.2$, 1, 5, 100, 200 and 500; from left to right. Dashed lines are the best fits of the data with the power-law function $n_{\mathrm{P}} \propto K^{\alpha_1}$ with $\alpha_1 \approx -2.6$, -2.47, -2.5, -1.98, -1.99, and -1.97 (from left to right). The dotted vertical line separates the slow diffusion regime ($K < 1$) from the quasilinear diffusion regime ($K \geqslant 1$).

remarkable overlap of the histograms into an universal curve. Moreover, we observe a small difference between the scaled histograms in the slow diffusion and the quasilinear diffusion regimes: The scaled values of n_{P} are slightly different; i.e., $n_{\mathrm{P}} K^{5/2}/h^2 \approx 2.4$ and $n_{\mathrm{P}} K^2/h^2 \approx 1.9$, respectively.

Finally, given that $P_{\mathrm{E}}(n)$ can be computed as the negative of the derivative of the survival probability with respect to n, it is possible to support the scaling (13) by our results for $P_{\mathrm{S}}(n)$ of the previous subsection as follows: using equation (11) we write

$$P_{\mathrm{E}}(n) = -\frac{dP_{\mathrm{S}}(n)}{dn} = \frac{\pi^2 D}{4\,h^2} \exp\left(-\frac{\pi^2 D}{4\,h^2} n\right). \tag{14}$$

Then, we make the change of variable $n \to \ln n$, which leads to $P_{\mathrm{E}}(\ln n) = nP_{\mathrm{E}}(n)$. Now, by defining n_p as the value of n for which $dP_{\mathrm{E}}(\ln n)/dn = 0$, i.e. the maxima of $P_{\mathrm{E}}(\ln n)$, we end up with $n_p = 4\,h^2/\pi^2 D$. This provides $n_{\mathrm{p}} \propto h^2$ and $n_{\mathrm{p}} \propto D^{-1}$ (that is $\alpha_1 = -z$; compare equations (10) and (13)), as numerically found above.

4. Conclusions

In this work, using an escape formalism, we have studied the behaviour of orbits in the phase space of a two-dimensional, nonlinear and area preserving, discontinuous mapping. The discontinuous map, parameterized by the control parameter K, presents two dynamical regimes (both diffusive) delimited by the critical value $K_c = 1$. Once a hole was defined in the phase space we concentrated on the diffusion coefficient D, the survival probability of particles $P_{\mathrm{S}}(n)$, and the histogram of escape times $P_{\mathrm{E}}(\ln n)$.

Due to the absence of the KAM scenario for this mapping, stickiness is not observed in the dynamics leading to the clean exponential decay of the survival probability in both the slow diffusion ($K < K_c$) and the quasilinear diffusion ($K > K_c$) regimes. Also, we demonstrated that $P_{\mathrm{E}}(\ln n)$ and $P_{\mathrm{S}}(n)$ are scale invariant with scaling laws proportional to the

diffusion coefficients of the corresponding dynamical regimes, namely, $D \propto K^{5/2}$ for $K < K_c$ and $D \propto K^2$ for $K > K_c$. We stress that the power-law dependencies of the diffusion coefficient on the parameter K that we found from the solution of the diffusion equation are in perfect agreement with previous studies on this map and other discontinuous maps [12, 14, 19].

The escape formalism used here can be extended to other dynamical systems described by discrete and discontinuous mappings.

Acknowledgments

JAMB acknowledges support from VIEP-BUAP (Grant No. MEBJ-EXC15-I), Fondo Institucional PIFCA (Grant No. BUAP-CA-169), CONACyT (Grants No. I0010-2014-246246 and No. CB-2013-220624), and FAPESP (Grant No. 2013/14655-9). JAMB also thanks FAPESP (Grant No. 2014/25997-0) for supporting a visit to Departamento de Matemática Aplicada e Estatística, Instituto de Ciências Matemáticas e de Computação, Universidade de São Paulo, Brazil, where this paper was written. ALPL thanks support from CNPq and FAPESP (2014/25316-3). EDL thanks support from FAPESP (2012/23688-5), CNPq and FUNDUNESP, Brazilian agencies.

References

[1] Altmann E G, Portela J S E and Tél T 2013 *Mod. Rev. Phys.* **85** 869
[2] Livorati A L P, Kroetz T, Dettmann C P, Caldas I L and Leonel E D 2012 *Phys. Rev.* E **86** 036203
[3] Dettmann C P and Leonel E D 2012 *Physica* D **241** 403
[4] Bunimovich L A and Dettmann C P 2005 *Phys. Rev. Lett.* **94** 100201
[5] Knight G, Georgiou O, Dettmann C P and Klages R 2012 *Chaos* **22** 023132
[6] Georgiou O, Dettmann C P and Altmann E G 2012 *Chaos* **22** 043115
[7] Livorati A L P, Georgiou O, Dettmann C P and Leonel E D 2014 *Phys. Rev.* E **89** 052913
[8] Gaspard P 1998 *Chaos, Scattering and Statistical Mechanics* (Cambridge: Cambridge University Press)
[9] Chirikov B V 1971 Institute of Nuclear Physics, Novosibirsk Preprint 267
Chirikov B V 1971 *CERN Trans.* 71–40 (Engl. trans.)
[10] Lichtenberg A J and Lieberman M A 1992 *Regular and Chaotic Dynamics* (New York: Springer-Verlag)
[11] Chirikov B V 1979 *Phys. Rep.* **52** 263
[12] Borgonovi F 1998 *Phys. Rev. Lett.* **80** 4653
[13] Mendez-Bermudez J A and Aguilar-Sanchez R 2012 *Phys. Rev.* E **85** 056212
[14] Borgonovi F, Casati G and Li B 1996 *Phys. Rev. Lett.* **77** 4744
[15] Casati G and Prosen T 1999 *Phys. Rev.* E **59** R2516
[16] Casati G and Prosen T 2000 *Phys. Rev. Lett.* **85** 4261
[17] Prosen T and Znidaric M 2001 *Phys. Rev. Lett.* **87** 114101
[18] Casati G and Prosen T 1999 *Phys. Rev. Lett.* **83** 4729
[19] Dana I, Murray N W and Percival I C 1989 *Phys. Rev. Lett.* **62** 233
[20] Greene J M 1979 *J. Math. Phys.* **20** 1183
[21] MacKay R S 1983 *Physica* D **7** 283
[22] MacKay R S, Meiss J D and Percival I C 1984 *Physica* D **13** 55
[23] MacKay R S and Percival I C 1985 *Comm. Math. Phys.* **94** 469
[24] Pathria R K 2008 *Statistical Mechanics* (Burlington: Elsevier)
[25] Gaspard P and Nicolis G 1990 *Phys. Rev. Lett.* **65** 1693
[26] Gaspard P and Alonso Ramirez D 1992 *Phys. Rev.* A **45** 8383
[27] deOliveira J A, Dettmann C P, daCosta D R and Leonel E D 2013 *Phys. Rev.* E **87** 062904